Design of Automatic Landing Systems using the H-inf Control and the Dynamic Inversion

Romulus Lungu
University of Craiova, Electrical, Energetic, and Aerospatiale Engineering Department
107 Decebal Street, 200440 Craiova, Romania
romulus_lungu@yahoo.com

Mihai Lungu[1]
University of Craiova, Electrical, Energetic, and Aerospatiale Engineering Department
107 Decebal Street, 200440 Craiova, Romania
Lma1312@yahoo.com

ABSTRACT

The paper focuses on the automatic control of aircraft in the longitudinal plane, during landing, by using the linearized dynamics of aircraft, taking into consideration the wind shears and the errors of the sensors. A new robust automatic landing system is obtained by means of the H-inf control, the dynamic inversion, an optimal observer and two reference models providing the aircraft desired velocity and altitude. The theoretical results are validated by numerical simulations for a Boeing 747 landing; the simulation results are very good (Federal Aviation Administration accuracy requirements for Category III are met) and show the robustness of the system even in the presence of wind shears and sensor errors. Moreover, the designed control law has the ability to reject the sensor measurement noises and wind shears with low intensity.

INTRODUCTION

For aircraft landing, the Automatic Landing Systems (ALSs) are used; most aircraft have ALSs based on the Instrumental Landing System (ILS) [1], using different conventional control laws (proportional-derivative – PD, proportional-integral – PI, proportional -integral-derivative - PID) for the altitude and descent velocity control [2-4], PD or PID conventional

[1] Corresponding author

laws for the pitch angle and pitch rate control. In recent years lots of researchers have applied the intelligent concepts for the automatic landing of the aircraft: the optimal synthesis $H_2, H_\infty, H_2/H_\infty$ [5, 6], the adaptive synthesis based on dynamic inversion theory and neural networks theory [7, 8], sliding mode control [9] or fuzzy techniques [10, 11]. In the area of optimal synthesis, Shue and Agarwal [12] have developed a mixed technique for the H_2/H_∞ control of landing, while Ochi and Kanai [13] have used the H_∞ control technique to design aircraft automatic approach and landing. In these papers, the authors did not analyze the robustness of the designed controllers in the presence of sensor errors and wind shears – issue which is considered in our paper. Other methods to design the control for aircraft landing involve the use of neural networks [14], but the weakness of these methods is that they do not control the aircraft to track the desired flight path accurate.

This paper focuses on the automatic control of aircraft in the longitudinal plane, during landing, by using the linearized longitudinal dynamics of aircraft, taking into consideration the longitudinal and vertical wind shears and the errors of the sensors. A new landing control system is designed by using the H-inf control and the dynamic inversion concept. Our new automatic landing system has some additional elements with respect to the one presented in [5]: an optimal observer, a block modeling the landing geometry and two reference models.

AIRCRAFT LONGITUDINAL DYNAMICS

The linearized dynamics used in our paper belongs to a Boeing 747 flight. The dynamics of aircraft motion, in longitudinal plane, is described by the state equation [2, 3]:

$$\dot{\boldsymbol{x}} = A\boldsymbol{x} + B\boldsymbol{u} + G\boldsymbol{u}_w, \tag{1}$$

with $\boldsymbol{x} \in R^{7\times1}-$ state vector, $\boldsymbol{x}=\begin{bmatrix} u & w & q & \theta & H & \delta_e & \delta_T \end{bmatrix}^T, \boldsymbol{u}=\begin{bmatrix} \delta_{ec} & \delta_{Tc} \end{bmatrix}^T \in R^{2\times1}-$ command vector, while $\boldsymbol{u_w}=\begin{bmatrix} V_{vx} & V_{vz} \end{bmatrix}^T \in R^{2\times1}$ is the vector of disturbances; V_{vx} and V_{vz} are the components of the wind velocity along the aircraft longitudinal and vertical [5]; u is the longitudinal velocity, w - vertical velocity, q – pitch angular rate, $\theta-$ pitch angle, H – aircraft altitude, while δ_e and δ_T are the elevator deflection and the thrust command, respectively; δ_{ec} and δ_{Tc} are the commands applied to elevator and engine, respectively. The matrices $A \in R^{7\times7}, B \in R^{7\times2}$ and $G \in R^{7\times2}$ are, respectively [15]:

$$A=\begin{bmatrix} a_{11} & a_{12} & 0 & a_{14} & 0 & b_{11} & b_{12} \\ a_{21} & a_{22} & a_{23} & 0 & 0 & b_{21} & b_{22} \\ a_{31} & a_{32} & a_{33} & 0 & 0 & b_{31} & b_{32} \\ 0 & 0 & 1 & 0 & 0 & 0 & 0 \\ 0 & a_{52} & 0 & a_{54} & 0 & 0 & 0 \\ 0 & 0 & 0 & 0 & 0 & -1/T_e & 0 \\ 0 & 0 & 0 & 0 & 0 & 0 & -1/T_T \end{bmatrix}, B=\begin{bmatrix} 0 & 0 \\ 0 & 0 \\ 0 & 0 \\ 0 & 0 \\ 0 & 0 \\ 1/T_e & 0 \\ 0 & 1/T_T \end{bmatrix}, G=\begin{bmatrix} -a_{11} & -a_{12} \\ -a_{21} & -a_{22} \\ -a_{31} & -a_{32} \\ 0 & 0 \\ 0 & 0 \\ 0 & 0 \\ 0 & 0 \end{bmatrix}. \quad (2)$$

The landing procedure involves three phases: initial approach, glide slope, and flare [16]. During initial approach, the pilot descends from the cruise altitude to 420 m above the ground (for Boeing 747). At 4 nautical miles from the runway, the glide slope path signal is intercepted; the pitch, attitude and speed must be controlled while the aircraft maintains a constant speed; for Boeing 747 the pitch angle is between -5 and 5 deg. At 30 m above the ground, the slope angle control system is disengaged and a flare maneuver is executed.

The equation associated to the glide slope phase ($H \geq H_0$, H_0- the altitude at which the glide slope phase ends) is $H_c=\left(X-X_{p_0}\right)\tan\left(\gamma_c\right), \dot{X}=u\cos\theta+w\sin\theta,$ where X is the covered horizontal distance, X_{p_0} is the coordinate of the point where the glide slope intersects the horizontal axis, H_c- the calculated flight altitude, while $\gamma_c=-2.5\text{deg}$ is the imposed slope angle during the first stage of landing. The equation

associated to the flare is $H_c = H_0 \exp(-t/\tau)$, with $\tau -$ time constant.

In (1) $\boldsymbol{u}_w$ is associated to a stochastic process defined by means of the velocities' spectrum; the velocities may be modeled using generator filters [4] with white noise input type. Here, the disturbances are the wind shears, their model being described by the equations [5]: $V_{vx} = -V_{vx_0}\sin(\omega_0 t), V_{vz} = -V_{vz_0}[1-\cos(\omega_0 t)], \omega_0 = 2\pi/T_0$, where T_0 is the flight time period inside the wind shear, while V_{vx_0} and V_{vz_0} are the maximum absolute values of the wind velocities with respect to longitudinal and vertical axes, respectively.

DESIGN OF THE AUTOMATIC LANDING SYSTEM

Consider the vector $z = \begin{bmatrix} H & u \end{bmatrix}^T = C'\boldsymbol{x}$ that contains the system controllable output variables, while the vector $\bar{z} = \begin{bmatrix} \bar{H} & \bar{u} \end{bmatrix}^T$ contains the imposed values of the flight altitude and longitudinal velocity. The output vector (*y*), in the absence of sensor errors, has the form $y = \begin{bmatrix} H & \dot{H} & u & \dot{u} & \theta & q \end{bmatrix}^T = C\boldsymbol{x}$. If the sensor errors are taken into account, the output vector is $y = C\boldsymbol{x} + D_{22}e$, where *e* is the vector containing the sensor errors, while D_{22} is a positive defined matrix; the matrices C and C' can be easily deduced.

Using $\bar{z}$ and the dynamic inversion principle, we calculate $\bar{x}$ (the desired state of the system) and $\bar{\boldsymbol{u}}$ (the desired control) with respect to $\bar{z}$ and, after that, the vector $\bar{y}$ is obtained by means of the equations: $\dot{\bar{\boldsymbol{x}}} = A\bar{\boldsymbol{x}} + B\bar{\boldsymbol{u}}, \bar{z} = C'\bar{\boldsymbol{x}}, \bar{y} = C\bar{\boldsymbol{x}}$. The command law is calculated with the formula: $\boldsymbol{u} = \bar{\boldsymbol{u}} + \boldsymbol{u}_\infty$, where $\boldsymbol{u}_\infty$ is the optimal command calculated by means of the H-inf method, while $\bar{\boldsymbol{u}}$ is calculated by using the dynamic inversion.

If the state equation (1), the equations of the variables $z_1 = H, z_2 = u$, and the equation are put together, the following equation is obtained:

$$\begin{bmatrix} \dot{\boldsymbol{x}} \\ z_1 \\ z_2 \\ y \end{bmatrix} = \begin{bmatrix} A_{(7\times7)} & B_{(7\times2)} & G_{(7\times2)} & 0_{(7\times6)} \\ C_{0(1\times7)} & D_{01(1\times2)} & 0_{(1\times2)} & 0_{(1\times6)} \\ C_{1(1\times7)} & D_{11(1\times2)} & 0_{(1\times2)} & 0_{(1\times6)} \\ C_{(6\times7)} & 0_{(6\times2)} & 0_{(6\times2)} & D_{22(6\times6)} \end{bmatrix} \begin{bmatrix} \boldsymbol{x} \\ \boldsymbol{u} \\ \boldsymbol{u_w} \\ e \end{bmatrix}; \tag{3}$$

A, B, G are (2), $C_0 = \begin{bmatrix} 0 & 0 & 0 & 0 & 1 & 0 & 0 \end{bmatrix}, C_1 = \begin{bmatrix} 1 & 0 & 0 & 0 & 0 & 0 & 0 \end{bmatrix}, D_{01} = \begin{bmatrix} c_1 & 0 \end{bmatrix}, D_{11} = \begin{bmatrix} c_2 & 0 \end{bmatrix}$, c_1 and c_2 are positive constants, while $D_{22} = k \cdot I_6$ is the weights' matrix for the vector containing the sensor errors $e = \begin{bmatrix} e_H & e_{\dot{H}} & e_u & e_{\dot{u}} & e_\theta & e_q \end{bmatrix}^T$; k is a small positive constant.

The optimal control law is of form [15]: $\boldsymbol{u}_\infty = -K_\infty (\hat{\boldsymbol{x}} - \bar{\boldsymbol{x}}), K_\infty = R_1^+ B^T P_\infty, R_1 = D_{11}^T D_{11}$; K_∞ is the controller gain matrix, while $\boldsymbol{u}_\infty$ minimizes the cost functional:

$$J = \frac{1}{2}\int_0^\infty z_2^T z_2 \mathrm{d}t = \frac{1}{2}\int_0^\infty \left[\boldsymbol{x}^T \underbrace{\left(C_1^T C_1\right)}_{Q_1} \boldsymbol{x} + \boldsymbol{u}_\infty^T \underbrace{\left(D_{11}^T D_{11}\right)}_{R_1} \boldsymbol{u}_\infty \right] \mathrm{d}t. \tag{4}$$

The symmetric and positive defined matrix $P_\infty \in R^{7\times7}$ is the solution of the Riccati matriceal equation: $A^T P_\infty + P_\infty A - P_\infty \left(B R_1^{-1} B^T - \mu_1^{-2} G G^T\right) P_\infty + Q_1 = 0$. To obtain the system estimated state $(\hat{\boldsymbol{x}})$ and $\Delta\hat{\boldsymbol{x}} = \hat{\boldsymbol{x}} - \bar{\boldsymbol{x}}$, we use the observer [15]: $\Delta\dot{\hat{\boldsymbol{x}}} = A\Delta\hat{\boldsymbol{x}} + B\boldsymbol{u} + L_\infty (\Delta y - C\Delta\hat{\boldsymbol{x}})$. The observer gain matrix $L_\infty \in R^{7\times6}$ is calculated by using the formula:

$$L_\infty = P_\infty^* C^T \left(D_{22}^T D_{22}\right)^{-1}, \tag{5}$$

with P_∞^* – solution of the Riccati equation [12]: $A P_\infty^* + P_\infty^* A^T - P_\infty^* \left(C^T C - \mu_2^{-2} Q_1\right) P_\infty^* + G G^T = 0$.

To obtain the values of the relative degrees for altitude H and for the aircraft longitudinal velocity u (r_1 and r_2, respectively), we differentiate the equations of $\dot{u}$ and $\dot{w}$ such that some terms containing the components of the control law $(\delta_{ec}, \delta_{Tc})$ appear in the expressions of the variables $\ddot{u}$ and $\ddot{w}$; it results some terms containing the variables $\dot{\delta}_{ec}$ and $\dot{\delta}_{Tc}$; these can be expressed by means of actuator's equations: $\dot{\delta}_e = -\frac{1}{T_e}\delta_e + \frac{1}{T_e}\delta_{ec}$,

$\dot{\delta}_T = -\frac{1}{T_T}\delta_T + \frac{1}{T_t}\delta_{Tc}$; we obtain $\ddot{u}$ and $\dddot{w}$ as functions of δ_{ec}, δ_{Tc}, and other states. Thus, the relative degree of the state u is $r_2 = 2$. In order to obtain the relative degree of the altitude (H), we differentiate the differential equation associated to H, i.e. $\dot{H} = a_{52}w + a_{54}\theta$, and we obtain $\ddot{H} = a_{52}\dot{w} + a_{54}\dot{\theta}$. Then, this is done again and $\dddot{H}$ is obtained. Therefore, the relative degree of the altitude is $r_1 = 3$. The following equations result:

$$\begin{aligned}
\ddot{u} &= a'_{11}u + a'_{12}w + a'_{13}q + a'_{14}\theta + a'_{16}\delta_e + a'_{17}\delta_T + \frac{b_{11}}{T_e}\delta_{ec} + \frac{b_{12}}{T_T}\delta_{Tc} + g'_{11}V_{vx} + g'_{12}V_{vz} + g_{11}\dot{V}_{vx} + g_{12}\dot{V}_{vz}, \\
\dddot{H} &= a'_{51}u + a'_{52}w + a'_{53}q + a'_{54}\theta + a'_{56}\delta_e + a'_{57}\delta_T + \frac{a_{52}b_{21}}{T_e}\delta_{ec} + \frac{a_{52}b_{22}}{T_T}\delta_{Tc} + g'_{51}V_{vx} + g'_{52}V_{vz} + g''_{51}\dot{V}_{vx} + g''_{52}\dot{V}_{vz},
\end{aligned} \tag{6}$$

with

$$\begin{aligned}
&g_{11} = -a_{11}, g_{12} = -a_{12}, g_{21} = -a_{21}, g_{22} = -a_{22}, g_{31} = -a_{31}, g_{32} = -a_{32}, a'_{11} = a_{11}^2 + a_{12}a_{21}, a'_{12} = a_{11}a_{12} + a_{12}a_{22}, \\
&a'_{13} = a_{12}a_{23} + a_{14}, a'_{14} = a_{11}a_{14}, a'_{16} = a_{11}b_{11} + a_{12}b_{21} - \frac{b_{11}}{T_e}, a'_{17} = a_{11}b_{12} + a_{12}b_{21} - \frac{b_{12}}{T_T}, g'_{11} = a_{11}g_{11} + a_{12}g_{21}, \\
&g'_{12} = a_{11}g_{12} + a_{12}g_{22}, a'_{51} = a_{54}a_{31} + a_{52}\left(a_{21}a_{11} + a_{21}a_{12} + a_{23}a_{31}\right), a'_{52} = a_{54}a_{32} + a_{52}\left(a_{21}a_{12} + a_{22}^2 + a_{23}a_{32}\right), \\
&a'_{53} = a_{54}a_{33}, a'_{54} = a_{52}\left(a_{22}a_{23} + a_{22}a_{33} + a_{21}a_{14}\right), a'_{56} = a_{52}\left(a_{21}b_{11} + a_{22}b_{21} + a_{23}b_{31} - \frac{1}{T_e}b_{21}\right) + a_{54}b_{31}, \\
&a'_{57} = a_{54}b_{32} + a_{52}\left(a_{21}b_{12} + a_{22}b_{22} + a_{23}b_{32} - \frac{1}{T_T}b_{22}\right), g'_{51} = a_{54}g_{31} + a_{52}\left(a_{21}g_{11} + a_{22}g_{21} + a_{23}g_{31}\right), \\
&g'_{52} = a_{54}g_{32} + a_{52}\left(a_{21}g_{12} + a_{22}g_{22} + a_{23}g_{32}\right), g''_{51} = a_{52}g_{21}, g''_{52} = a_{52}g_{22}.
\end{aligned} \tag{7}$$

The equations $\dot{\bar{\boldsymbol{x}}} = A\bar{\boldsymbol{x}} + B\bar{\boldsymbol{u}}, \bar{z} = C'\bar{\boldsymbol{x}}, \bar{y} = C\bar{\boldsymbol{x}}$ may be combined into a single one (equation of the vector $z^{(r)} = \left[\dddot{H} \quad \ddot{u}\right]^T$); we obtain the form of the control law $\bar{\boldsymbol{u}}$ if we impose the convergence of $z^{(r)} = \left[\dddot{H} \quad \ddot{u}\right]^T$ to $\bar{z}^{(r)} = \left[\overline{\dddot{H}} \quad \overline{\ddot{u}}\right]^T$ and of the system estimated state $(\hat{\boldsymbol{x}})$ to $\boldsymbol{x}$; we get: $\bar{\boldsymbol{u}} = B_u^{-1}\left(\bar{z}^{(r)} - A_x\hat{\boldsymbol{x}} - G'\boldsymbol{u}_w - G''\ddot{\boldsymbol{u}}_w\right) = h_r^{-1}\left(\bar{z}^{(r)}, \hat{\boldsymbol{x}}, \boldsymbol{u}_w\right)$, with

$$B_u = \begin{bmatrix} \frac{a_{52}b_{21}}{T_e} & \frac{a_{52}b_{22}}{T_T} \\ \frac{b_{11}}{T_e} & \frac{b_{12}}{T_T} \end{bmatrix}, A_x = \begin{bmatrix} a'_{51} & a'_{52} & a'_{53} & a'_{54} & 0 & a'_{56} & a'_{57} \\ a'_{11} & a'_{12} & a'_{13} & a'_{14} & 0 & a'_{16} & a'_{17} \end{bmatrix}, G' = \begin{bmatrix} g'_{51} & g'_{52} \\ g'_{11} & g'_{12} \end{bmatrix}, G'' = \begin{bmatrix} g''_{51} & g''_{52} \\ g''_{11} & g''_{12} \end{bmatrix}. \tag{8}$$

The structure of the new automatic landing system, using the dynamic inversion and the H-inf method, is presented in Fig. 1. The vectors $\bar{z}$ and $\bar{z}^{(r)}$ are provided by two reference models, the former being a three order reference model, while the latter is a second order reference model (Fig. 2) [15]. The obtaining of the aircraft desired landing trajectory involves two variables' control: the forward speed (u) and the altitude (H).

NUMERICAL SIMULATION RESULTS

To study the performances of the new automatic landing system, we consider the landing of a Boeing 747. Complex simulations in Matlab/Simulink have been performed; thus, we designed the optimal observer, the H-inf controller, and, after that, we validated the proposed automatic landing system. The values of the coefficients for Boeing 747 dynamics have been borrowed from [5]. The elements of matrix G have been calculated with (2); the vector e is $e=\left[1\text{m}\quad 1\text{deg/s}\quad 1\text{m}\quad 0\text{m/s}^2\quad 1\text{deg}\quad 1\text{deg/s}\right]^T$, while, for the reference models, we have chosen: $p=25,\xi_1=\xi_2=0.7,\omega_1=\omega_2=2\text{rad/s}$. For the first landing phase, we also used the values: $H_p=H(0)=420\text{m},X(0)=0,X_{p_0}=-H_p/\tan(\gamma_c),\gamma_c=-2.5\text{deg}$.

In Fig. 3 and Fig. 4 we represent the time histories for the glide slope landing phase and flare landing phase, respectively; the characteristics have been represented for the ALS affected by wind shears in the presence or in the absence of sensor errors (the sensors are used for the measurement of the states). The last four mini-graphics in Figs. 3 and 4 represent the deviations of the forward speed (u), sink rate $(\dot{H})$, slope angle (γ), and altitude (H), with respect to their nominal values, i.e. $u-\bar{u},\dot{H}-\bar{\dot{H}}$, $\gamma-\gamma_c,H-\bar{H}$. The presence of the sensor errors is not visible: the curves with solid line

(obtained for the ALS without sensor errors) overlap almost perfectly over the curves plotted with dashed line (obtained for the ALS with sensor errors).

By analyzing Figs. 3 and 4, we remark the correctness of the simulation data. During the glide slope, the aircraft must have a linear descendent trajectory (8th graphic in Fig. 3) and, as a consequence, the pitch angle must be negative; as one can see in Fig. 3, the pitch angle is -2.55 degrees, while the attack angle is slightly negative $(\cong -0.05\deg)$; it results the desired slope angle (-2.5 degrees). In the flare phase, the aircraft must describe a parabolic trajectory (8th graphic in Fig. 4) with a null slope angle; indeed, the pitch and the attack angles become zero in about 30 seconds, resulting the desired null slope angle.

The landing begins at a longitudinal speed initially exceeding the nominal speed by 1 m/s (see the first graphic in Fig. 3). The speed is reduced to the normal speed (70 m/s) and then kept at this value. From last graphics in Figs. 3 and 4, we can also see that the final error between the desired path and the actual path is less than 0.3 m during the glide slope phase and 0 m for flare. These errors are very good if we analyze the Federal Aviation Administration (FAA) accuracy requirements for Category III (the best category) [17]; according to FAA Category III accuracy requirements, the vertical error must be less than 0.5 m, while the final altitude at the end of flare must be 0 m.

Above, the matrix D_{22} (the weights' matrix associated to the sensor errors) has been chosen as $D_{22} = k \cdot I_6$, where k is a small positive constant; for Figs. 3 and 4, we have used the value k=0.06, but it is interesting to see what happens if this constant is increased. A change of the matrix D_{22} is equivalent with a modification of the observer gain matrix L_∞; this means a modification of the observer errors and, accordingly, a modification of all the

variables' time history. We represent in Fig. 5 the time history of this error $\left(\overline{H}-H\right)$ for different values of D_{22}; for the first landing phase, the altitude error increases when the constant k is increased. For the second landing phase, the constant increase is equivalent with the increase of flare duration and horizontal covered distance (a serious problem because the distance which is required for a proper landing may exceed the runway length).

CONCLUSIONS

The robust ALS designed in this paper uses the H-inf control and the dynamic inversion taking into consideration the longitudinal and vertical wind shears and the errors of the sensors. The H-inf control provides robust stability with respect to the uncertainties caused by different disturbances and noise type signals, while the dynamic inversion provides good precision tracking. The ALS represents an improved version of the automatic landing system designed in [5] and it differs from other similar automatic landing systems from the specialty literature, being characterized by better tracking precision and a more general character. The simulation results are promising and show the robustness of the designed control system even in the presence of wind shears and sensor errors.

REFERENCES

[1] Donald, McL., 1990, "Automatic Flight Control Systems," Prentice Hall Publisher.

[2] Lungu, R., Lungu, M., Grigorie, T. L., 2012, "ALSs with conventional and fuzzy controllers considering wind shears and gyro errors," Journal of Aerospace Engineering, **26**(4), pp. 794-813.

[3] Lungu, R., Lungu, M., Grigorie, T. L., 2013, "Automatic control of aircraft in longitudinal plane during landing," IEEE Transactions on Aerospace & Electronic Systems, **49**(2), pp. 1338-1350.

[4] Juang, J. G., Cheng, K.C., 2006, "Application of Neural Network to Disturbances Encountered Landing Control," IEEE Transactions on Intelligent Transportation Systems, **7**(4), pp. 582-588.

[5] Che, J., Chen, D., 2001, "Automatic Landing Control using H_∞ control and Stable Inversion," Proceedings of the 40th Conference on Decision and Control, Orlando, Florida, USA, pp. 241-246.

[6] Li, Y., Sundararajan, N., Saratchandran, P., Wang, Z., 2004, "Robust neuro-H∞ controller design for

aircraft auto-landing," IEEE Transactions on Aerospace and Electronic Systems, **40**(1), pp. 158-167.

[7] Mori, R., Suzuki, S., 2009, "Neural Network Modeling of Lateral Pilot Landing Control." Journal of Aircraft, **46**, pp. 1721-1726.

[8] Vo, H., Sridhar, S., 2008, "Robust Control of F-16 Lateral Dynamics," International Journal of Aerospace and Mechanical Engineering, pp. 80-85.

[9] Rao, D.M., Go, T.H., 2014, "Automatic landing system design using sliding mode control," Aerospace Science and Technology, **32**, pp. 180-187.

[10] Zdenko, K., Stjepan, B., 2006, " Fuzzy Controller Design – Theory and applications," Taylor and Francis.

[11] Kumar, V. Rana, K.P., Gupta, V., 2008, "Real-Time Performance Evaluation of a Fuzzy PI + Fuzzy PD Controller for Liquid-Level Process," International Journal of Intelligent Control and Systems, **13**(2), pp. 89-96.

[12] Shue, S., Agarwal, R. K., 1999, "Design of automatic landing systems using mixed H_2/H_∞ control," Journal of Guidance, Control, and Dynamics, **22**(1), pp. 103-114.

[13] Ochi, Y., Kanai, K., 1999, "Automatic approach and landing for propulsion controlled aircraft by H_∞ control," Proceedings of the 1999 IEEE International Conference on Control Applications, Hawaii, pp. 997-1002.

[14] Afshari, H., Roshanian, J., Novinzadeh, A., 2011, "Robust Nonlinear Optimal Solution to the Lunar Landing Guidance by Using Neighboring Optimal Control," Journal of Aerospace Engineering, **24**(1), pp. 20-30.

[15] Lungu, M., 2008, "Sisteme de conducere a zborului (Flight control systems)," Sitech Publisher.

[16] Parkinson, B., O'Connor, M., Fitzgibbon, K., 1996, "Aircraft automatic approach and landing using GPS," Global Positioning System: Theory and Applications, vol. II, Cambridge, pp. 397-425.

[17] Braff, R., Powell, J.D., Dorfler, J., 1996, "Applications of GPS to air traffic control," Global Positioning System: Theory and Applications, vol. II, Cambridge, pp. 327-374.

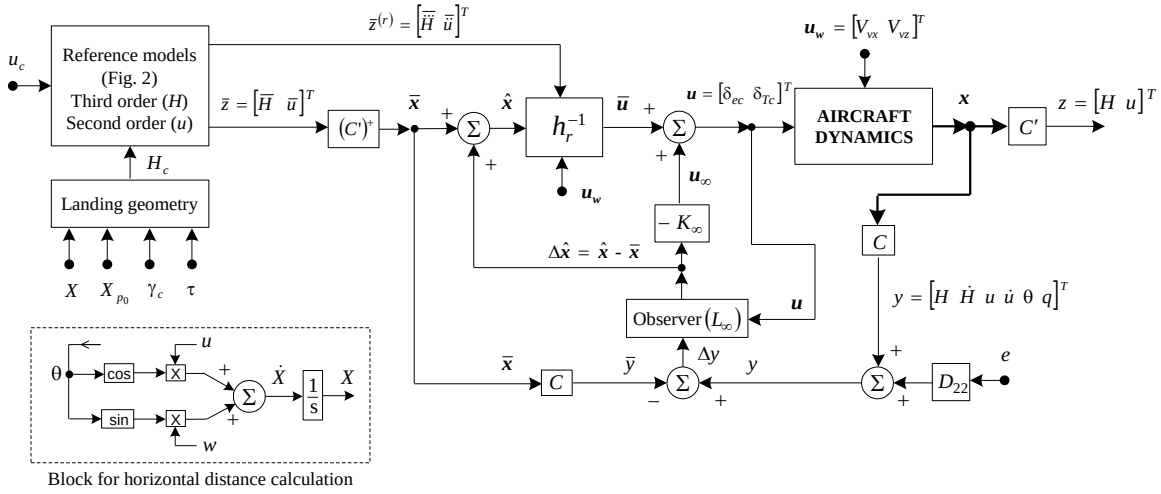

Fig. 1 New automatic landing system using dynamic inversion and H-inf method

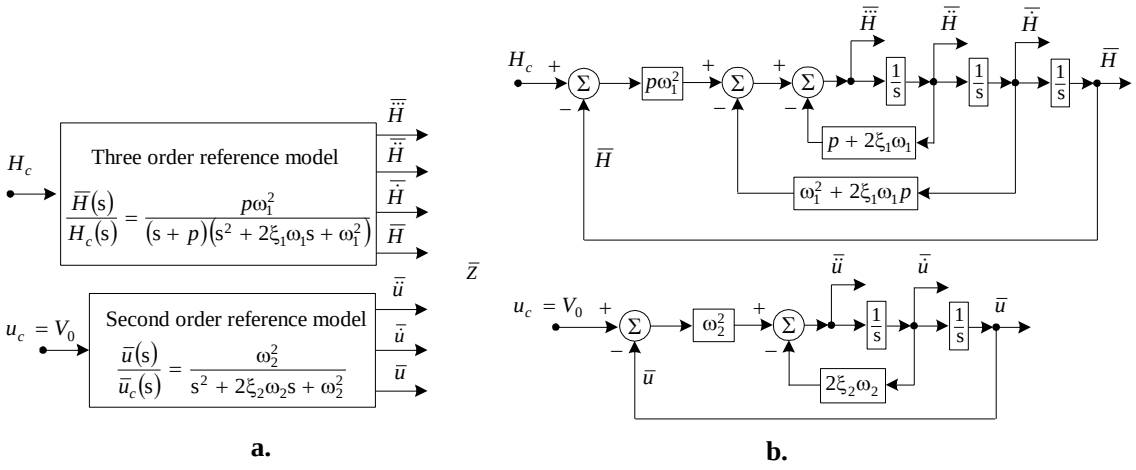

Fig. 2 Block diagrams of the three order and second order reference models, respectively: a) simplified block diagram; b) detailed block diagram

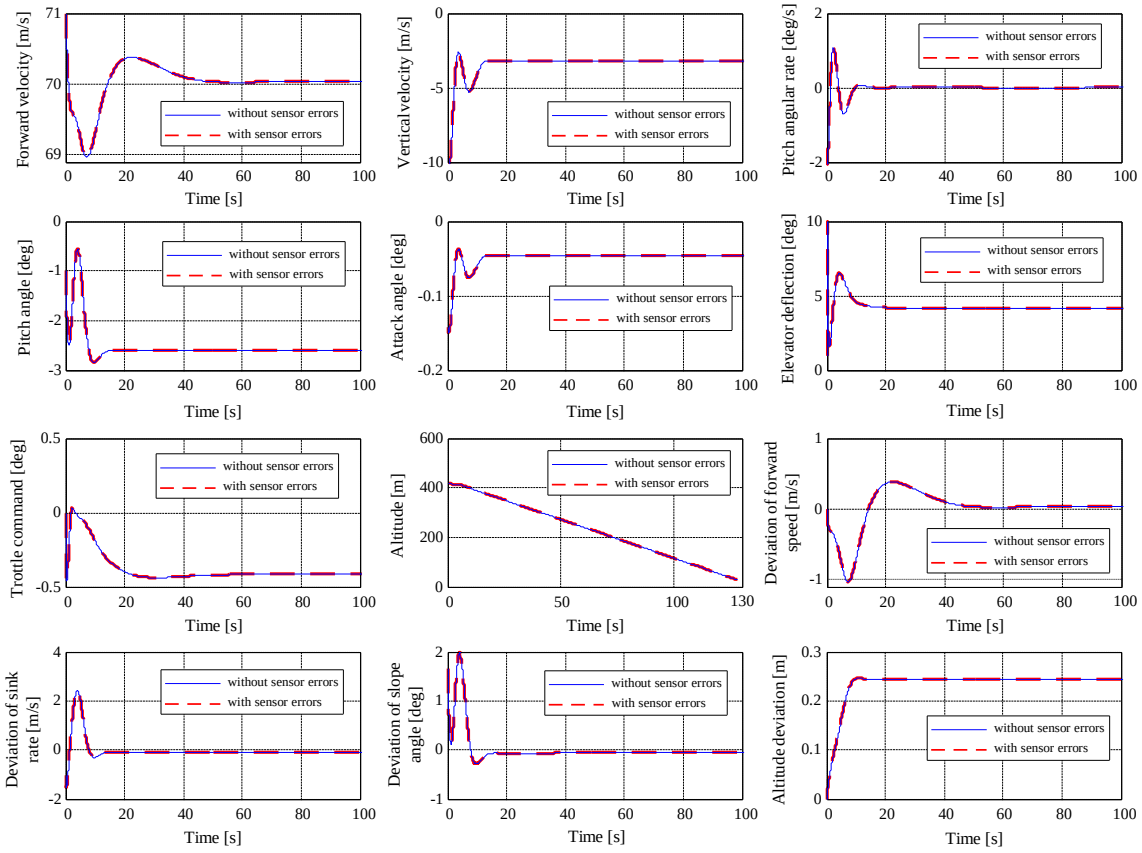

Fig. 3 Time characteristics for the glide slope phase, with or without sensor errors

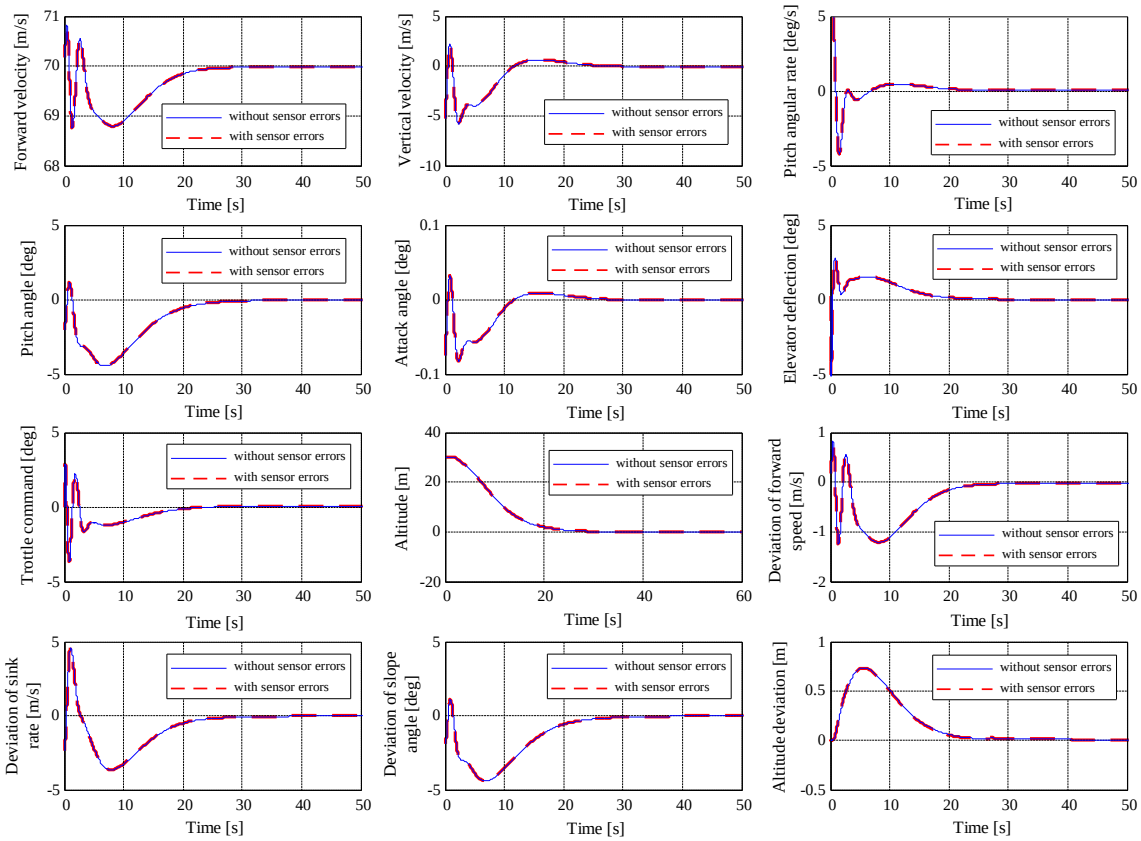

Fig. 4 Time characteristics for the flare phase, with or without sensor errors

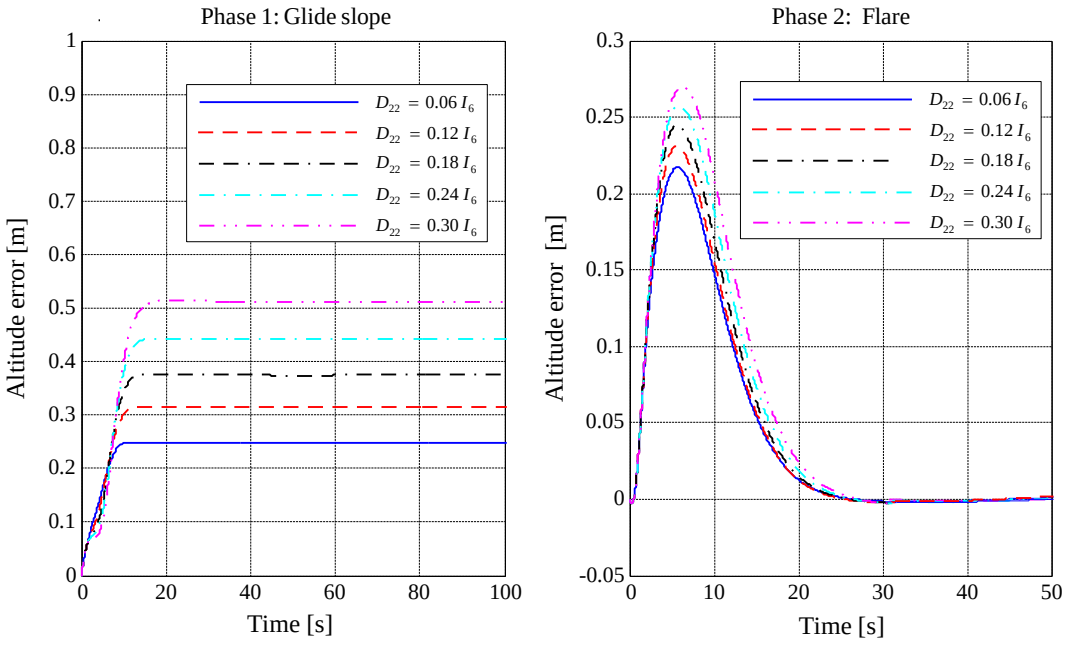

Fig. 5 Aircraft altitude errors for different values of matrix D_{22}